Electrodynamic forces driving DNA-enzyme interaction at a large distance

Elham Faraji, Philip Kurian, Roberto Franzosi, Stefano Mancini, Irena Cosic, Drasko Cosic, Giulio Pettini, Marco Pettini

Electrodynamic forces driving DNA-enzyme interaction at a large distance

Elham Faraji,[1,2,3,4,*] Philip Kurian,[5,†] Roberto Franzosi,[6,7,4,‡] Stefano Mancini,[1,4,§]
Irena Cosic,[8,¶] Drasko Cosic,[8,**] Giulio Pettini,[9,††] and Marco Pettini[2,3,‡‡]

[1]*School of Science and Technology, University of Camerino, I-62032 Camerino, Italy*

[2]*Aix Marseille Univ, Université de Toulon, CNRS, CPT, Marseille, France*

[3]*CNRS Centre de Physique Théorique UMR7332, 13288 Marseille, France*

[4]*INFN Sezione di Perugia, I-06123 Perugia, Italy*

[5]*Quantum Biology Laboratory, Howard University, Washington, DC 20060, USA*

[6]*DSFTA, University of Siena, Via Roma 56, 53100 Siena, Italy*

[7] *QSTAR and INO-CNR, largo Enrico Fermi 2, I-50125 Firenze, Italy*

[8]*AMALNA Consulting, Black Rock 3193, VIC, Australia*

[9] *Dipartimento di Fisica Università di Firenze, and I.N.F.N., Sezione di Firenze, via G. Sansone 1, I-50019 Sesto Fiorentino, Italy*

(Dated: May 24, 2022)

Abstract

In the present paper we address a model of DNA-protein selective interaction. The biochemical model is chosen on the basis of existing literature, both theoretical and experimental. This consists of a restriction enzyme, EcoRI, binding selectively to a 6 base-pair subsequence of an oligonucleotide to cleave it. A signature of the specific partnership of the two molecules is first obtained by applying the so-called Resonant Recognition Model. Then the same system is investigated by means of a model inspired to the standard Davydov and Holstein-Fröhlich models describing the electron motion along a biomolecule. Starting with a model Hamiltonian written in second quantization, the Time Dependent Variational Principle is used to work out the dynamical equations of the system. The time-Fourier spectra of the electron currents numerically computed for the DNA fragment and for the EcoRI enzyme, respectively, are multiplied to get a cross-spectrum which displays a sharp peak of co-resonance. The remarkable result is the replacement of this sharp peak with a broad and noisy frequency pattern when the recognition sequence GAATTC on the DNA is randomized. This sequence-dependent charge transfer phenomenology is suggestive of a potentially rich variety of selective electrodynamic interactions of DNA molecules and transcription factors under the action of electron excitation.

*Electronic address: elham.faraji2012@gmail.com

†Electronic address: pkurian@howard.edu

‡Electronic address: roberto.franzosi@unisi.it

§Electronic address: stefano.mancini@unicam.it

¶Electronic address: icosic@amalnaconsulting.com

**Electronic address: dcosic@amalnaconsulting.com

††Electronic address: pettini@fi.unifi.it

‡‡Electronic address: pettini@cpt.univ-mrs.fr

I. INTRODUCTION

Progress in molecular and cellular biology is consistently linked to a better knowledge of the structure of, and functional interplay between biomolecules such as DNA, RNA and proteins. Even though these building blocks of the living matter display no apparent systematic spatial order, it is well known that all the relevant biochemical processes follow precisely timed sequences, in other words display a dynamical order. DNA/RNA-interacting proteins (e.g., helicases, polymerases, nucleases, recombinases) modulate essential transaction processes involving nucleic acids to achieve DNA duplication and repair, gene expression and recombination, with an astonishing efficiency. Such an astonishing efficiency raises a fundamental question from a physical point of view. With biochemical reactions mostly being stereo specific, two (or more) reacting partners have to come in close contact and exhibit a definite spatial orientation to initiate particular reactions. Then, how do the various actors in a given biochemical process efficiently find each other (i.e., how does a protein effectively recruits the appropriate co-effector partner(s) or selectively connects with its DNA/RNA target(s) in a crowded cyto/nucleoplasm environment)? In other words, what are the physical forces that bring all these players at the right place, in the right order and in a reasonably short time to sustain cellular function and ultimately cellular life? The classical way to tackle these issues invokes Brownian motion (actually other proposals have been put forward, like facilitated diffusion, but these alternative explanations do not apply to bulk recruitment of molecules). At physiological temperature, ubiquitously distributed water molecules undergo chaotic motion, colliding with larger/heavier fluid components. On the latter, the neat outcome from simultaneous hits is a force of both random intensity and direction. Hence, large molecules move in a diffusive way throughout the cellular spaces and sooner or later shall encounter their cognate partners. Is this truly a good answer to the problem formulated here? Many doubts arise when one tries to estimate diffusion driven activation for some of the biochemical processes mentioned above, in fact free diffusion is considerably slowed down in the crowded cellular space [1]. Moreover, the discrepancy between the observed reaction rates in cells and the predictions of strict random diffusion modelling are being recently questioned [2–7]. Therefore, it is timely to reconsider a longstanding hypothesis, put forward in the 1960s by H. Fröhlich [8] who surmised that certain biochemical reactions could be accelerated by selective electrodynamic forces acting over long distances. This hypothesis would explain a number of phenomena in living matter, such as the extraordinary efficiency of enzymatic reactions [9], of the molecular

DNA transcription machinery, of certain ligand-receptor recruitments, and so on [10, 11]. For both technological and theoretical reasons, no formal confirmation (or refutation) of this hypothesis of electrodynamic interactions between biomolecules has been validated until recently. After a thorough theoretical revisitation of Fröhlich's theory [12], an experimental feasibility study [13, 14] and the experimental observation of an out-of-equilibrium phonon condensation in a model protein [15] which is a necessary condition [12] to activate intermolecular electrodynamic interactions, a first experimental evidence of the activation of these forces has been provided very recently [16].

Within this newly opened field, the aim of the present work is to investigate whether intermolecular electrodynamic interactions can be also put at work under different conditions of activation, but without giving up the ingredient of resonance, a crucial one for selective recruitment of the cognate partners of a biochemical reaction. To this aim we will combine and adapt the Resonant Recognition Model [17], detailed below, and a recent picture of intermolecular interactions as being mediated by water dipolar waves [18]. This paper is organized as follows. In Section II the RRM is quickly sketched and applied to the interaction of the EcoRI restriction enzyme with an oligonucleotide (a 66 base pairs double stranded DNA fragment) containing a cleavage sequence recognized by the enzyme. In Section III we define the model used to describe the electron motion along the DNA fragment and the enzyme separately. Section IV contains the definition of the physical parameters used in the numerical simulations of the model equations. The results of these numerical simulations are then reported in Section V. The possibility of activating water mediated DNA-EcoRI interaction is discussed in Section VI. Finally, in Section VII some concluding remarks are reported.

II. THE RESONANT RECOGNITION MODEL

The Resonant Recognition Model (RRM), which has been extensively published [17, 20–22], is based on discovery that crucial driving force for macromolecules (protein, DNA and RNA) activation and interaction is resonant electromagnetic energy transfer at specific frequency unique for specific activation and interaction. The RRM model is capable to calculate these frequencies from periodicities within the distribution of energy of delocalised electrons along protein, DNA and/or RNA molecules using charge velocity through these macromolecules. This concept has been applied on number of proteins, DNA and/or RNA examples [17, 20–23], as well as on some medical conditions like: Crigler-Najjar syndrome [24], pain [25] and influence of environmental light to

health [26]. This concept has been also experimentally tested by predicting the electromagnetic frequencies for activation of L-Lactate Dehydrogenase [27] and has been tested on experimental measurements of photon emission from dying melanoma cells [28], on photon emission from lethal and non-lethal Ebola strains [29], as well as on differentiation of osteoblasts stem cells [30]. These findings could be used, not only to understand biological processes and resonances in biomolecules, but also to influence these processes using either radiation or design of related molecules and conductive particles.

A. The RRM applied to the DNA-EcoRI model

In order to meet with the model considered in Refs.[18, 32], we have applied here the RRM model to analyse forces driving DNA-enzyme interaction between a 66bp oligonucleotide containing a cleavage subsequence of the EcoRI enzyme and EcoRI enzyme itself, as presented in Figure 1.

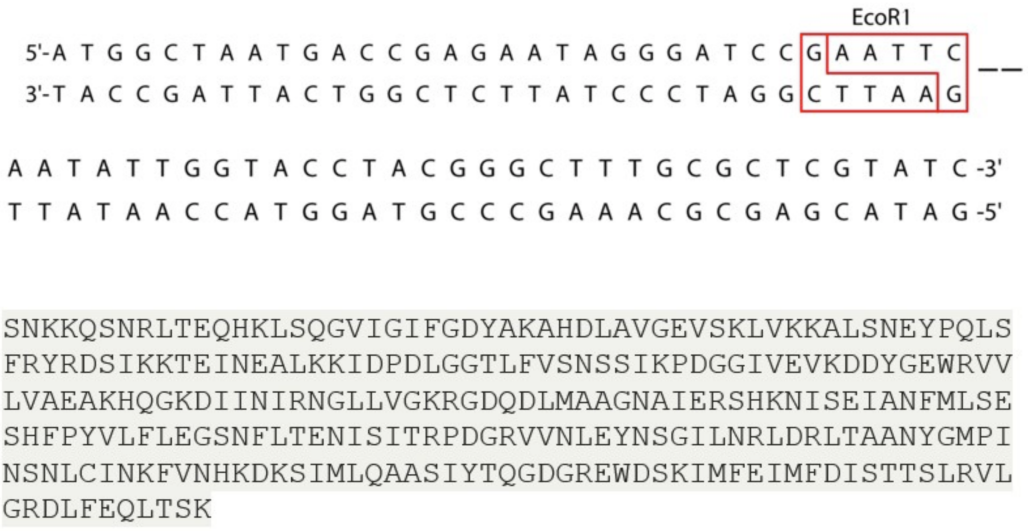

Figure 1: Top: Sequence of an oligonucleotide (66 bp) containing a cleavage subsequence of EcoRI enzyme. Bottom: amino acid sequence of EcoRI enzyme.

Through the RRM model it is possible to analyse interactions directly computationally between amino acid sequences (proteins) and nucleotide sequences (DNA and RNA), based only on matching frequencies within free electron energy distribution along these macromolecules. When we have applied the RRM model to compare 66bp oligonucleotide containing a cleavage subsequence

of the EcoRI enzyme and EcoRI enzyme, we have found very strong common RRM frequency at $f = 0.1699 \pm 0.0152$, indicating that this frequency is crucial for mutual interaction between 66bp oligonucleotide and EcoRI enzyme, as presented in Figure 2. Interestingly, we have also found that nucleotide pair C-G at the position 33, which is within the cleavage site of 66bp oligonucleotide is mostly contributing to RRM characteristic frequency at $f = 0.1699 \pm 0.0152$ and thus represent 'hot spot' [17, 20, 21] for this interaction. Furthermore, electromagnetic frequencies that correspond to RRM frequencies depend on velocity of charge through macromolecular backbone. For the velocity of 7.87×10^5m/s as proposed by RRM [17, 20, 21], the corresponding electromagnetic frequency for RRM frequency $f = 0.1699 \pm 0.0152$ would be from 160THz to 192THz.

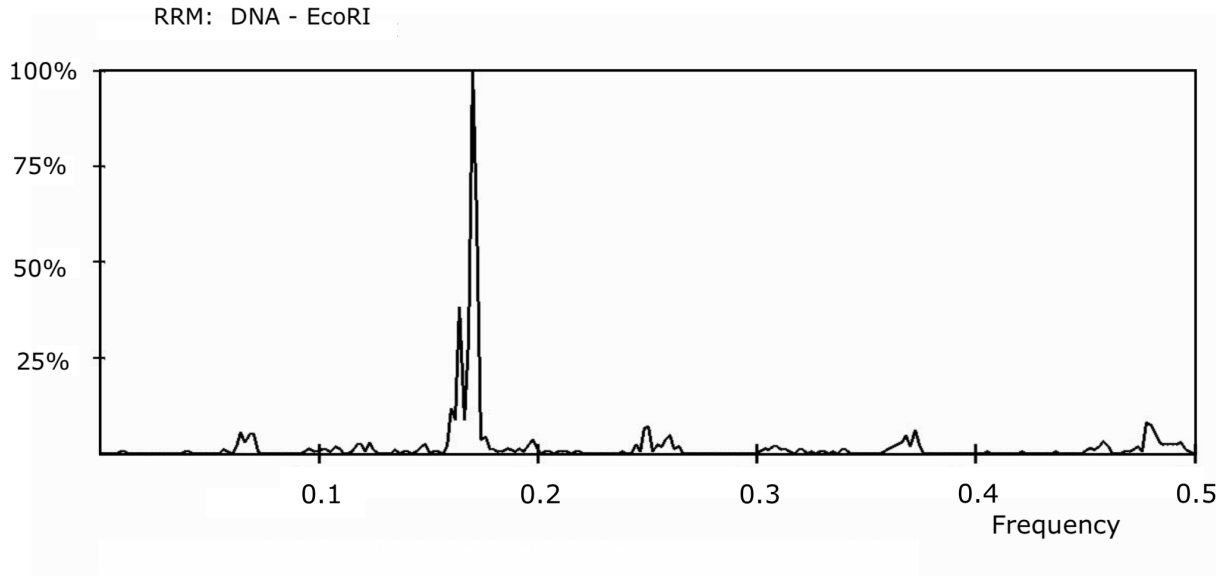

Figure 2: Characteristic RRM frequency for mutual interaction between 66bp oligonucleotide and EcoRI enzyme at $f = 0.1699 \pm 0.0152$

However, for the velocity of 1.2×10^5 m/s as proposed by Yomosa [31], the corresponding electromagnetic frequency for RRM frequency $f = 0.1699 \pm 0.0152$ would be from 24THz to 29THz, which is in accordance with the range of frequencies calculated in the next sections of this paper.

III. DEFINITION OF A DYNAMICAL MODEL AND ITS SOLUTION

In our recent work we found a rich phenomenology of intermolecular interactions of DNA molecules under the action of an external source of energy. Depending on the initial electron excitation site and excitation energy, we saw the concentrated periodic motions of the electrons arising a well-peaked frequency spectrum of the electron current to the motions with a spread noisy frequency spectrum. This motivated us strongly to interpret Resonant Recognition Model (RRM) with the aid of an explicit modelling of the electronic motions along the backbones of interacting DNA-protein biomolecules. In order to describe these electronic motions and their electrodynamic interactions we resort to a model partly borrowed from the standard Davydov and Holstein-Fröhlich models that have been originally introduced to account for electron-phonon interaction [33–35]. Thus, to model the electrons moving along a given DNA sequence and along the backbone of a DNA-interacting enzyme (we will consider the EcoRI restriction enzyme), separately, the following common Hamiltonian operator for both EcoRI enzyme and DNA is assumed

$$\hat{H} = \hat{H}_{el} + \hat{H}_{ph} + \hat{H}_{int}, \tag{1}$$

with

$$\hat{H}_{el} = \sum_{n=1}^{N} \Big[E_0 \hat{B}_n^\dagger \hat{B}_n + \epsilon \langle \hat{B}_n^\dagger \hat{B}_n \rangle \hat{B}_n^\dagger \hat{B}_n + J_n (\hat{B}_n^\dagger \hat{B}_{n+1} + \hat{B}_n^\dagger \hat{B}_{n-1}) \Big], \tag{2}$$

$$\hat{H}_{ph} = \frac{1}{2} \sum_{n} \Big[\frac{\hat{p}_n^2}{M_n} + \Omega_n (\hat{u}_{n+1} - \hat{u}_n)^2 + \frac{1}{2} \mu (\hat{u}_{n+1} - \hat{u}_n)^4 \Big], \tag{3}$$

$$\hat{H}_{int} = \sum_{n} \chi_n (\hat{u}_{n+1} - \hat{u}_n) \hat{B}_n^\dagger \hat{B}_n. \tag{4}$$

in which $\hat{H}_{el}$ and $\hat{H}_{ph}$ are respectively the electronic and phononic Hamiltonians and $\hat{H}_{int}$ indicates the electron-phonon interaction term. The coupling parameters are assumed dependent on the electron excitation site with respect to the site-independent case [36]. Considering only a longitudinal chain of amino acids (or nucleotides), $\hat{B}_n$ and $\hat{B}_n^\dagger$ denote the lowering and raising operators between the lattice site $n \in \{1, 2, \ldots, N\}$ labelling the amino acids along the EcoRI enzyme (or nucleotides along a DNA). The parameter E_0 implies the initial excitation energy of the electron according to the initial form of the electronic state vector. The nonlinear constant ϵ is the coupling energy of the interaction between the moving electron along the chain with the electrons of the substrate of amino acids (or nucleotides). The coupling parameter J_n is site-dependent tunnelling term of electron across two nearest neighbouring amino acids (or nucleotides).

The momentum and position operators $\hat{p}_n$ and $\hat{u}_n$ of the vibronic Hamiltonian determine the longitudinal displacements of the n-th phonon in the sequence of amino acids (or nucleotides) from their equilibrium position and the coupling term Ω_n denotes the site-dependent spring parameter of two neighbouring sites. M_n is the mass of the n-th amino acid of EcoRI enzyme sequence (or nucleotide of a DNA segment) and the nonlinear coupling constant μ implies phonon-phonon interaction, absent in the harmonic approximation. Finally, the parameter χ_n of the interaction Hamiltonian is the electron-phonon coupling dependent of the n-th site.
The wave function $|\psi(t)\rangle$ at any time t may be written in the Davydov ansatz by the following factorization

$$|\psi(t)\rangle = |\Psi(t)\rangle|\Phi(t)\rangle, \tag{5}$$

with the normalization condition $\langle\psi(t)|\psi(t)\rangle = 1$. The state vector $|\Psi(t)\rangle$ describes a single quantum excitation of electron propagating along a protein chain of N amino acids (or a DNA sequence of N nucleotides)

$$|\Psi(t)\rangle = \sum_n C_n(t)\hat{B}_n^\dagger|0\rangle_{el}, \tag{6}$$

in which $|0\rangle_e$ is the electronic vacuum state, and $|\Phi(t)\rangle$ is the vibronic wave function

$$|\Phi(t)\rangle = e^{-i/\hbar\sum[\beta_n(t)\hat{p}_n - \pi_n(t)\hat{u}_n]}|0\rangle_{ph}, \tag{7}$$

for which the expectation values for longitudinal displacement $\hat{u}_n$ and momentum $\hat{p}_n$ are respectively, $\langle\Phi|\hat{u}_n|\Phi\rangle = \beta_n(t)$ and $\langle\Phi|\hat{p}_n|\Phi\rangle = \pi_n(t)$. According to the time-dependent variation principle (TDVP), we define a phase factor ($S(t) \in \mathbb{R}$) and set a new wave function $|\phi(t)\rangle$ from Eq.(5) as $|\phi(t)\rangle = e^{iS(t)/\hbar}|\psi(t)\rangle$ satisfying the normalization $\langle\phi(t)|\phi(t)\rangle = 1$. Integrating the quantum Schrödinger equation, $i\hbar\langle\phi(t)|\partial_t|\phi(t)\rangle = \langle\phi(t)|\hat{H}|\phi(t)\rangle$ leads to $S(t) = \int_0^t L(t')dt'$ which can be supposed as the classical Lagrangian associated to the system

$$L(t) = i\hbar\langle\psi(t)|\partial_t|\psi(t)\rangle - \langle\psi(t)|\hat{H}|\psi(t)\rangle. \tag{8}$$

Now, TDVP which is equivalent to the least action principle reads as

$$\delta S(t) = \delta\int_0^t L(t')dt' = 0. \tag{9}$$

Then from the wave function (5) and Lagrangian (8) we have

$$L = \sum_n \left\{ i\hbar\dot{C}_n(t)C_n^*(t) + \frac{1}{2}\Big(\pi_n(t)\dot{\beta}_n(t) - \dot{\pi}_n(t)\beta_n(t)\Big) - H(C_n, C_n^*, \beta_n, \pi_n)\right\}, \tag{10}$$

in which $H(C_n, C_n^*, \beta_n, \pi_n) = \langle\psi(t)|\hat{H}|\psi(t)\rangle$. Here we fulfill the stationary action (9) and obtain

$$\begin{aligned}\delta S(t) \;=& \sum_n \Big\{ i\hbar\Big(- \dot{C}_n^*(t)\delta C_n(t) + \dot{C}_n(t)\delta C_n^*(t)\Big) + \dot{\beta}_n(t)\delta\pi_n(t) - \dot{\pi}_n(t)\delta\beta_n(t) \\ & -(\partial_{C_n}H)\delta C_n - (\partial_{C_n^*}H)\delta C_n^* - (\partial_{\beta_n}H)\delta\beta_n - (\partial_{\pi_n}H)\delta\pi_n\Big\} = 0, \end{aligned} \tag{11}$$

which gives the equations

$$\begin{aligned} i\hbar\dot{C}_n &= \partial_{C_n^*}H \\ \dot{\beta}_n &= \partial_{\pi_n}H \\ \dot{\pi}_n &= -\partial_{\beta_n}H. \end{aligned} \tag{12}$$

According to the expectation value of the Hamiltonian

$$\begin{aligned}\langle\psi|\hat{H}|\psi\rangle \;=& \sum_n \Big[E_0|C_n|^2 + \epsilon|C_n|^4 + J_n(C_n^*C_{n+1} + C_{n+1}^*C_n) \\ & +\tfrac{1}{2}\Big(\tfrac{1}{M_n}\pi_n^2 + \Omega_n(\beta_{n+1}-\beta_n)^2 + \tfrac{1}{2}\mu(\beta_{n+1}-\beta_n)^4\Big) \\ & +\chi_n(\beta_{n+1}-\beta_n)|C_n|^2\Big]. \end{aligned} \tag{13}$$

and Eqs. (12) the equations of the motion are found as

$$\begin{aligned} i\hbar\dot{C}_n &= \Big(E_0 + 2\epsilon|C_n|^2 + \chi_n(\beta_{n+1}-\beta_n)\Big)C_n + J_nC_{n+1} + J_{n-1}C_{n-1}, \\ M_n\ddot{\beta}_n &= \Omega_n\beta_{n+1} + \Omega_{n-1}\beta_{n-1} - \Omega_{n-1}\beta_n - \Omega_n\beta_n + \chi_n|C_n|^2 - \chi_{n-1}|C_{n-1}|^2 \\ &+ \mu\Big((\beta_{n+1}-\beta_n)^3 - (\beta_n-\beta_{n-1})^3\Big). \end{aligned} \tag{14}$$

It is worth noting that the dynamical equations worked out by means of the TDVP are formally classical but give the time evolution of actual quantum expectation values.

IV. PHYSICAL PARAMETERS FOR THE NUMERICAL COMPUTATIONS

We need to determine the physical and authentic values of the coupling parameters of the Hamiltonian to do our numerical simulations. In so doing, we borrow the quantities from Ref.[37, 38] of the potential interaction energies between an electron and each of all the amino acids reported in table I as well as the potential energies of the interaction between an electron

Nucleotide	EIIP Ry	EIIP eV	Nucleotide	EIIP Ry	EIIP eV
A	0.1260	1.7143	T	0.1335	1.8164
G	0.0806	1.0966	C	0.1340	1.8232

Table I: Electron-Ion interaction potential (EIIP) values for nucleotides adenine (A), thymine (T), guanine (G), and cytosine (C). From Ref.[37].

Amino acid	EIIP Ry	EIIP eV	Amino acid	EIIP Ry	EIIP eV
Leu	0.0000	0.0000	Tyr	0.0516	0.7017
Ile	0.0000	0.0000	Trp	0.0548	0.7452
Asn	0.0036	0.0489	Gln	0.0761	1.0349
Gly	0.0050	0.0680	Met	0.0823	1.1192
Val	0.0057	0.0775	Ser	0.0829	1.1274
Glu	0.0058	0.0788	Cys	0.0829	1.1274
Pro	0.0198	0.2692	Thr	0.0941	1.2797
His	0.0242	0.3291	Phe	0.0946	1.2865
Lys	0.0371	0.5045	Arg	0.0959	1.3042
Ala	0.0373	0.5072	Asp	0.1263	1.7176

Table II: Electron-Ion interaction potential (EIIP) value for 20 amino acids. From Ref.[37].

with each of four nucleotides presented in table II. The electron in motion with the initial energy E_0, during its route, experiences a periodic sequence of square potential barriers of different height and of the same width a - the average distance between two nearest neighboring sites - by tunneling across the chain of amino acids constituting a protein or the sequence of nucleotides composing DNA. Such a distance is $a = 4.5\mathring{A}$ and $a = 3.4\mathring{A}$ respectively in EcoRI enzyme and DNA fragment. Then we can estimate roughly the electron tunneling term as $J_n = E_0 T_{n,n+1}$ by introducing the transmission coefficient $T_{n,n+1}$ from the probability $P(n \to n \pm 1)$ of tunneling from one potential barrier to the nearest one as follows

- Case 1: $E_0 < E_{n+1}$

$$T_{n,n+1} = \left[1 + \frac{E_{n+1}^2 \sinh^2(\beta_{n+1} a)}{4E_0(E_{n+1} - E_0)}\right]^{-1}, \tag{15}$$

where $\beta_{n+1} = [2m_e(E_{n+1} - E_0)/\hbar^2]^{1/2}$.

- Case 2: $E_0 > E_{n+1}$

$$T_{n,n+1} = \left[1 + \frac{E_{n+1}^2 \sin^2(\beta_{n+1} a)}{4E_0(E_0 - E_{n+1})}\right]^{-1}, \tag{16}$$

in which $\beta_{n+1} = [2m_e(E_0 - E_{n+1})/\hbar^2]^{1/2}$.

Here m_e is the mass of electron and E_{n+1} are the potential interaction energies between the electrons in motion and the local amino acids (or nucleotides). Moreover, in a rough estimation we set $\chi_n = dE/dx = (E_{n+1} - E_n)/a$ as the site-dependent electron-phonon coupling.
In order to perform the numerical simulations, the dimensionless expectation value of the Hamitonian (13) and of the dimensionless equations of motion (14) are found by rescaling time $t = \omega^{-1}\tau$ and length $\beta_n = Lb_n$ where $L = (\hbar\omega^{-1}M_n^{-1})^{1/2}$. Then we obtain

$$\begin{aligned}\langle\psi|\hat{H}|\psi\rangle = \sum_n \Big[& E'|C_n|^2 + \epsilon'|C_n|^4 + J'_n(C_n^* C_{n+1} + C_{n+1}^* C_n) \\ & + \frac{1}{2}\Big(\dot{b}_n^2 + \Omega'_n(b_{n+1} - b_n)^2 + \frac{1}{2}\mu'(b_{n+1} - b_n)^4\Big) \\ & + \chi'_n(b_{n+1} - b_n)|C_n|^2\Big],\end{aligned} \tag{17}$$

and

$$\begin{aligned} i\frac{dC_n}{d\tau} &= \Big(E' + 2\epsilon'|C_n|^2 + \chi'_n(b_{n+1} - b_n)\Big)C_n + J'_n C_{n+1} + J'_{n-1}C_{n-1}, \\ \frac{d^2 b_n}{d\tau^2} &= \Omega'_n b_{n+1} + \Omega'_{n-1}b_{n-1} - \Omega'_{n-1}b_n - \Omega'_n b_n + \chi'_n|C_n|^2 - \chi'_{n-1}|C_{n-1}|^2 \\ &+ \mu'\Big[(b_{n+1} - b_n)^3 - (b_n - b_{n-1})^3\Big], \end{aligned} \tag{18}$$

where the dimensionless parameters are

$$\begin{aligned} E' &= \frac{E_0}{\hbar\omega}; \qquad \epsilon' = \frac{\epsilon}{\hbar\omega}; \qquad J'_n = \frac{J_n}{\hbar\omega}; \\ \chi'_n &= \frac{\chi_n}{\sqrt{\hbar M_n \omega^3}}; \qquad \Omega'_n = \frac{\Omega_n}{M_n\omega^2}; \qquad \mu' = \frac{\mu\hbar}{M_n^2\omega^3}\,. \end{aligned} \tag{19}$$

The sound speed of amino acids is $V \sim 4$ Km/s from [33, 40] and of nucleotides is $V = 1.69$ Km/s from [39] (neglecting small local variations due to the different masses of the amino acids or the nucleotides). We apply two different analyzes for computing the spring parameter in our simulations. First, we consider the known speed of sound $V = a(\Omega_n/M_n)^{1/2}$ leading to the constant dimensionless parameter $\Omega' = V^2/a^2\omega^2$ from (19) where $\Omega' = 0.79$ for amino acids and $\Omega' = 0.25$ for nucleotides. Second, from [33] we borrow the spring constant of amino acids $\Omega = 18.3N/m$ giving us from (19) the site-dependent dimensionless $\Omega'_n = 1.83/m_n$. Third, we

assume the average spring constant $\Omega = V^2\langle M\rangle/a^2$ of DNA -in which $\langle M\rangle$ is the average masses of the nucleotides- and acquire the dimensionless site-dependent parameter $\Omega'_n = 0.48/m_n$ for nucleotides. The expression m_n represents the dimensionless mass of amino acids and nucleotides. In order to perform numerical integration of the dynamical equations it is useful to introduce the variables

$$q_n = \frac{C_n + C_n^*}{\sqrt{2}}, \qquad p_n = \frac{C_n - C_n^*}{i\sqrt{2}}, \tag{20}$$

then we rewrite Eqs.(18) as

$$\dot{q}_n = \Big[E' + \frac{\epsilon'}{2}(q_n^2 + p_n^2) + \chi'(b_{n+1} - b_n)\Big]p_n + J'_n p_{n+1} + J'_{n-1}p_{n-1}, \tag{21}$$

$$\dot{p}_n = -\Big[E' + \frac{\epsilon'}{2}(q_n^2 + p_n^2) + \chi'(b_{n+1} - b_n)\Big]q_n + J'_n q_{n+1} + J'_{n-1}q_{n-1}\Big], \tag{22}$$

$$\begin{aligned}\ddot{b}_n = {} & \Omega'(b_{n+1} + b_{n-1} - 2b_n) + \frac{1}{2}\Big(\chi'_n(q_n^2 + p_n^2) - \chi'_{n-1}(q_{n-1}^2 + p_{n-1}^2)\Big) \\ & + \mu'\Big[(b_{n+1} - b_n)^3 - (b_n - b_{n-1})^3\Big].\end{aligned} \tag{23}$$

Substituting the r.h.s of above equation (23) with $\mathscr{B}_n[\mathbf{b}(t), \mathbf{q}(t), \mathbf{p}(t)]$ reads as $b_n(t + \Delta t) = 2b_n(t) - b_n(t - \Delta t) + (\Delta t)^2\mathscr{B}_n[\mathbf{b}(t), \mathbf{q}(t), \mathbf{p}(t)]$; therefore

$$\begin{aligned}\dot{b}_n &= \pi_n \\ \dot{\pi}_n &= \mathscr{B}_n[\mathbf{b}(t), \mathbf{q}(t), \mathbf{p}(t)]\ .\end{aligned} \tag{24}$$

Furthermore, we denote $\mathscr{Q}_n[\mathbf{b}(t), \mathbf{q}(t), \mathbf{p}(t)]$ and $\mathscr{P}_n[\mathbf{b}(t), \mathbf{q}(t), \mathbf{p}(t)$ respectively with the r.h.s. of Eqs.(21) and (22) and obtain the numerical integrations by combining a finite differences scheme and a leap-frog scheme as follows

$$\begin{aligned}q_n(t + \Delta t) &= q_n(t) + \Delta t\ \mathscr{Q}_n[\mathbf{b}(t), \mathbf{q}(t), \mathbf{p}(t)], \\ p_n(t + \Delta t) &= p_n(t) + \Delta t\ \mathscr{P}_n[\mathbf{b}(t), \mathbf{q}(t), \mathbf{p}(t), \\ b_n(t + \Delta t) &= b_n(t) + \Delta t\ \pi_n(t), \\ \pi_n(t + \Delta t) &= \pi_n(t) + \Delta t\ \mathscr{B}_n[\mathbf{b}(t + \Delta t), \mathbf{q}(t + \Delta t), \mathbf{p}(t + \Delta t)].\end{aligned} \tag{25}$$

The integration scheme for $b_n(t)$ and $p_n(t)$ is a symplectic one, meaning that all the Poincaré invariants of the associated Hamiltonian flow are conserved, among these invariants there is energy. We can not apply the simple leap-frog scheme to the equations for $\dot{q}_n(t)$ and $\dot{p}_n(t)$ due to the r.h.s. of the equations for $\dot{q}_n(t)$ explicitly depend on $q_n(t)$ and $b_n(t)$; therefore, we integrate the first two

equations in (25) with an Euler predictor-corrector to arrive

$$
\begin{aligned}
q_n^{(0)}(t+\Delta t) &= q_n(t) + \Delta t\ \mathscr{Q}_n[\mathbf{b}(t), \mathbf{q}(t), \mathbf{p}(t)], \\
p_n^{(0)}(t+\Delta t) &= p_n(t) + \Delta t\ \mathscr{P}_n[\mathbf{b}(t), \mathbf{q}(t), \mathbf{p}(t)], \\
q_n^{(1)}(t+\Delta t) &= q_n(t) + \frac{\Delta t}{2}\left\{\mathscr{Q}_n[\mathbf{b}(t), \mathbf{q}(t), \mathbf{p}(t)] + \mathscr{Q}_n[\mathbf{b}(t), \mathbf{q}^{(0)}(t+\Delta t), \mathbf{p}^{(0)}(t+\Delta t)]\right\}, \\
p_n^{(1)}(t+\Delta t) &= p_n(t) + \frac{\Delta t}{2}\left\{\mathscr{P}_n[\mathbf{b}(t), \mathbf{q}(t), \mathbf{p}(t)] + \mathscr{P}_n[\mathbf{b}(t), \mathbf{q}^{(0)}(t+\Delta t)), \mathbf{p}^{(0)}(t+\Delta t)]\right\}, \\
b_n(t+\Delta t) &= b_n(t) + \Delta t\ \pi_n(t), \\
\pi_n(t+\Delta t) &= \pi_n(t) + \Delta t\ \mathscr{B}_n[\mathbf{b}(t+\Delta t), \mathbf{q}^{(1)}(t+\Delta t), \mathbf{p}^{(1)}(t+\Delta t)].
\end{aligned}
\tag{26}
$$

The integration of half of the set of the dynamical equations (25) by means of a symplectic algorithm, and half of the equations by means of the Euler predictor-corrector (26) results in the very well conservation of total energy without any shift- just with zero-mean fluctuations around a given value fixed by the initial conditions- by considering sufficiently small integration time steps Δt. We need also to define the initial states of electron and phonon independently of the specific physical excitation mechanism. The electron wavefunction (6) is described by the amplitudes $C_n(t=0)$ centered at the excitation site $n = n_0$ and distributed at time $t = 0$ [33] as

$$
C_n(t=0) = \frac{1}{\sqrt{8\sigma_0}}\mathrm{sech}\Big(\frac{n-n_0}{4\sigma_0}\Big) \tag{27}
$$

where σ_0 specifies the amplitude width. Concerning the phonon part of the system, we consider a thermalized macromolecule EcoRI enzyme and DNA fragment at room temperature $T = 310^{\circ}K$. At thermal equilibrium, average kinetic and potential energies per degree of freedom are equal, and the total energy is equally shared among all the phonon modes. Accordingly, the displacements and the associated velocities have been initialized with random values of zero-mean at $t = 0$, then in a dimensionless form we have

$$
\langle|b_n(0)|\rangle_n = \sqrt{\frac{k_B T}{\hbar\omega\Omega'}}; \qquad\qquad \langle|\pi_n(0)|\rangle_n = \sqrt{\frac{k_B T}{\hbar\omega}}. \tag{28}
$$

Periodic boundary conditions have been used for the both electron and phonon part of the DNA-EcoRI interacting system and the frequency has been assumed $\omega = 10^{13}\mathrm{s}^{-1}$.

V. NUMERICAL RESULTS

We have used an integration time step $\Delta t = 5 \times 10^{-6}$ to work out our numerical simulations with a very good energy conservation and the typical relative error $\Delta E/E = 10^{-6}$. The following

analyses have reported the spectral properties of electron currents in the interaction of a DNA fragment of $N = 66$ nucleotides and an EcoRI restriction enzyme of $N = 276$ amino acids for the different initial activation energies of electron E_0, the various initial excitation sites of electron n_0 of the probability amplitude (27) and the distinct forms of the phononic spring term Ω_n. We study the Fourier spectrum of the electron current activated on a segment of DNA and also DNA-interacting enzyme, separately and, from now on, use the index 1 and 2 for all the terms of DNA and EcoRI, respectively. Resorting to the standard probability current $j(x,t)$ of the electron wave function (6) the electron density current is given by

$$j(x,t) = \frac{e\hbar}{2m_e i}\left(\psi^\star \nabla\psi - \psi\nabla\psi^\star\right)$$

hence the average electron current, in a spatially discretized form for numerical computation, is

$$\begin{aligned} i_{1,2}(t) \;&=\; \frac{1}{l_{1,2}}\int_0^{l_{1,2}} j_{1,2}(x,t)dx = \frac{e\hbar}{2N_{1,2}a_{1,2}m_e i} \\ &\times \sum_{j=1}^{N_{1,2}}\Big(\Psi^*_{1,2}(x_j,t)\frac{\Psi_{1,2}(x_{j+1},t)-\Psi_{1,2}(x_{j-1},t)}{2} \\ &-\; \Psi_{1,2}(x_j,t)\frac{\Psi^*_{1,2}(x_{j+1},t)-\Psi^*_{1,2}(x_{j-1},t)}{2}\Big), \end{aligned} \tag{29}$$

where $l_{1,2}$ are the lengths, and $i_{1,2}$ are the currents flowing along the DNA fragment and the EcoRI enzyme macromolecules, respectively. In Figures. (3) and (5), we have plotted the cross Fourier spectrum of the currents $\tilde{i}^*_1(\nu)\tilde{i}_2(\nu)$ of DNA containing the sites CTTAAG, recognized by the enzyme EcoRI, and studied whether they are specific sites, which has a fundamental role in the DNA-protein interaction. Fig. (3) shows the behavior of the system when the excited electron on the DNA has the initial energy $E_{1,0} = 0.72$ eV and its wavefunction is initially centered at the site $n_{1,0} = N/2$, while for the restriction enzyme the initial excitation energy of the electron is $E_{2,0} = 0.2$ eV localized at $n_{2,0} = N/3$. Besides, as we discussed already in Section IV, we consider the dimensionless expressions of the site-dependent phononic spring $\Omega'_{1,n} = 0.48/m_n$ for the nucleotides and the constant term $\Omega'_2 = 0.79$ for the amino acids. We see the very interesting phenomenon of a clear co-resonance around 20 THz when the specific CTTAAG restriction sequence is taken into account. This result is in qualitative agreement, and possibly also in very good quantitative agreement as discussed in Section II, with the peak found by applying the RRM. Another significant finding is that the cross spectrum becomes completely spread when the recognition sites are randomly chosen AGCTTA. Moreover, when we exchange just one nucleotide of

the restriction sequence with its own complementary as CATAAG the co-resonance undergoes a little alteration and broadens by changing two nucleotides of the recognition sites in the form of GTTAAC. In Figure (5) the results are reported as numerical simulations obtained for the different initial conditions which confirm well the robustness of the phenomenology previously seen. Here we assume the initial electronic activation energy $E_{1,0} = 0.85$ eV posited in the site $n_{1,0} = N/2$ in DNA macromolecule and the ones in the DNA-interacting enzyme $E_{2,0} = 0.85$ eV located in $n_{2,0} = N/3$. Also, the dimensionless parameter of phononic spring in DNA fragment is assumed constant $\Omega_1' = 0.25$ and in EcoRI enzyme is considered site-dependent $\Omega_{2,n}' = 1.83/m_n$. The sharp peak of co-resonant spectrum of the DNA-EcoRI interaction with the characteristic site restriction sites CTTAAG happens around 29 THz that broads entirely by choosing the randomized recognition sites TCATGA. It is clear that the sharp frequency spectrum ramifies very little by exchanging only one nucleotide of the sites, cleaved by EcoRI, with its complementary as CTTATG and destroys somehow more when two nucleotides are exchanged with their complementary sites as CTATAG

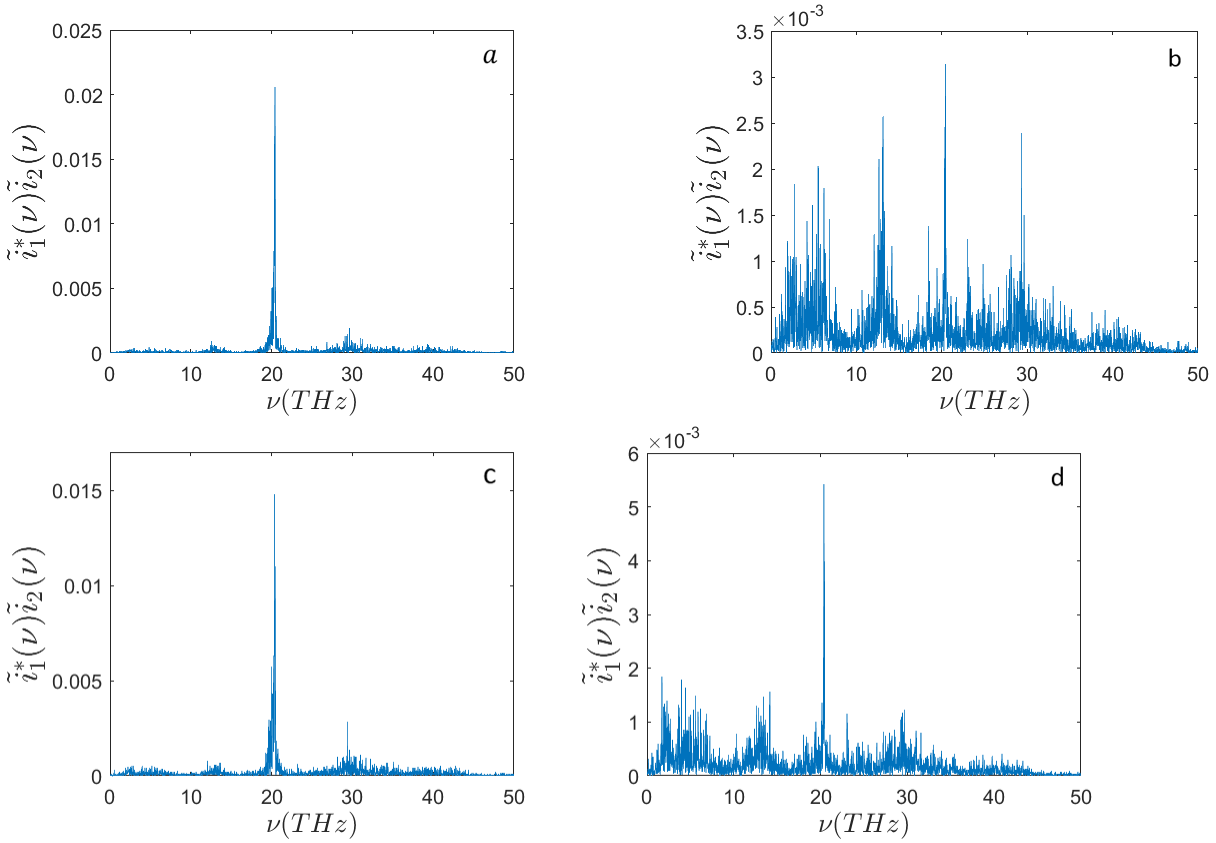

Figure 3: The cross frequency spectrum of the interaction between DNA strand with $N_1 = 66$ nucleotides and the EcoRI enzyme with $N_2 = 276$ amino acids for the initial conditions: $T = 310°K$, $N_{0,1} = N/2$, $N_{0,2} = N/3$, $E'_{1,0} = 110$, $E'_{2,0} = 30$, $\epsilon'_1 = \epsilon'_2 = 5$, $\mu'_1 = \mu'_2 = 0.5$, $\Omega'_2 = 0.79$ and site-dependent parameters $\Omega_{1,n} = 0.48/m_n$, $J'_{1,n}$, $J'_{2,n}$, $\chi'_{1,n}$ and $\chi'_{2,n}$ corresponding to $E_{0,1} = 0.72$ eV, $E_{0,2} = 0.2$ eV, $\epsilon_1 = \epsilon_2 = 0.0329$ eV, $\mu_1 = \mu_2 = 0.5$, $\Omega_{2,n} = V^2\langle M\rangle/a^2$, $\Omega_{1,n} = V^2 M_n/a^2$, $J_{1,n}$, $J_{2,n}$, $\chi_{1,n}$ and $\chi_{2,n}$ regarding to the Equations (15) and (16); and $\sigma_{1,0} = \sigma_{2,0} = 0.1$. a) DNA containing the specific CTTAAG recognition sites, b) randomized restriction sites AGCTTA, c) exchanging only one nucleotide with its complementary CATAAG, d) exchanging two nucleotides with their complementaries GTTAAC.

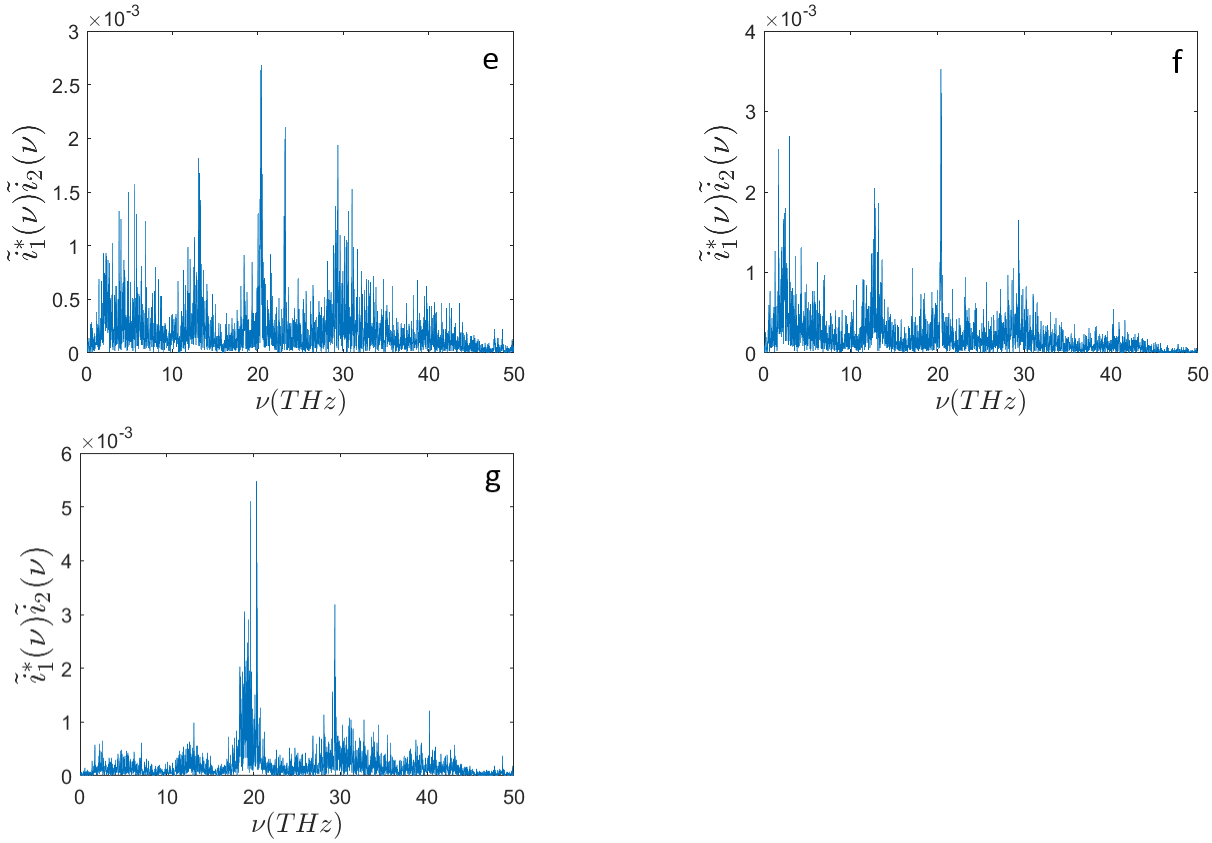

Figure 4: Same physical conditions of Figure 3. The cross frequency spectrum of the interaction between DNA and the EcoRI enzyme. e) The randomized restriction sites TCATGA, f) exchanging only one nucleotide with its complementary CTTAAC, g) exchanging two nucleotides with their complementaries CATATG. The frequency ν is measured in $10^{13}\mathrm{s}^{-1}$.

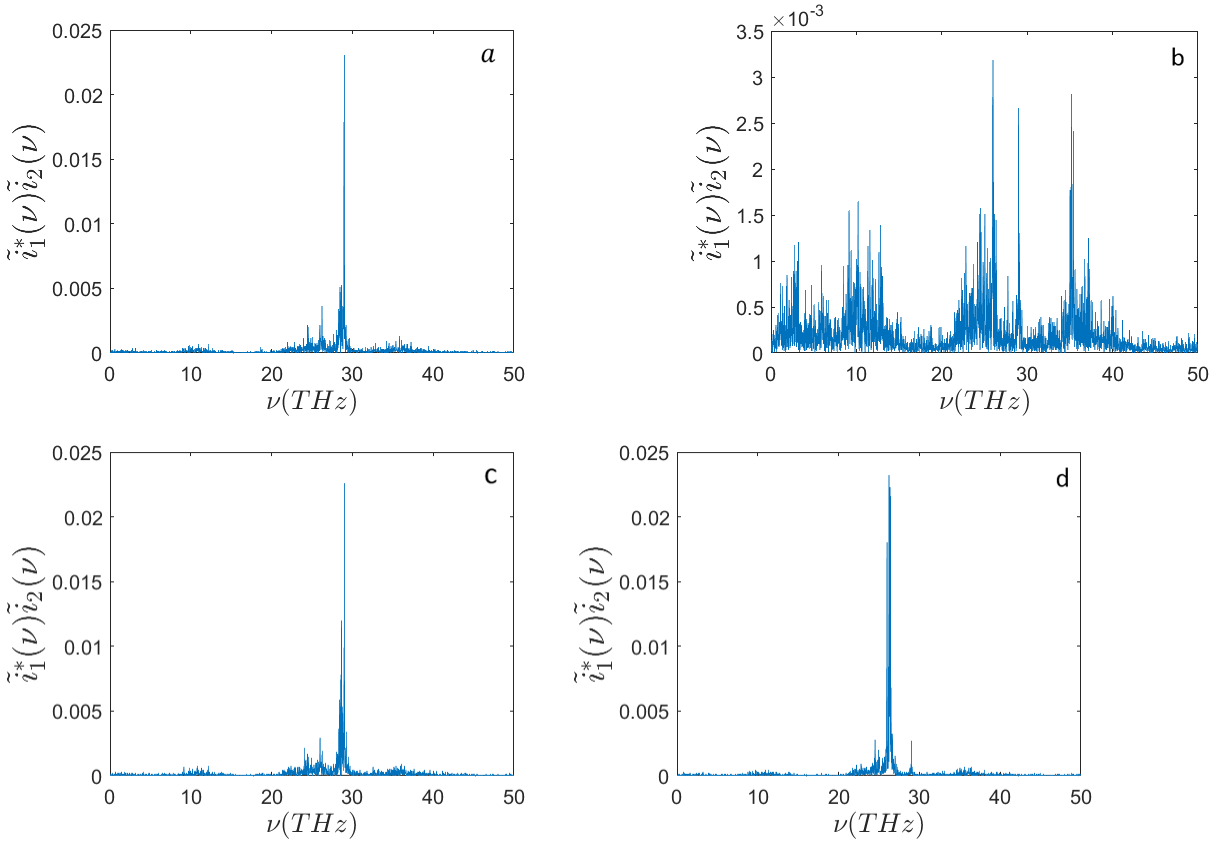

Figure 5: The cross frequency spectrum of the interaction between DNA strand with $N_1 = 66$ nucleotides and the EcoRI enzyme with $N_2 = 276$ amino acids for the initial conditions: $N_{0,1} = N/2$, $N_{0,2} = N/3$, $E'_{1,0} = E'_{2,0} = 129.17$, $\Omega'_{1,n} = 0.25$, $\Omega'_{2,n} = 1.83/m_n$ corresponding to $E_{1,0} = E_{2,0} = 0.85$ eV, $\Omega_{1,n} = V^2 M_n/a^2$ and $\Omega_2 = 18.3$ N/m. The other parameters are the same as Figure (3); a) DNA containing the specific recognition sites CTTAAG, b) randomized restriction sites TCATGA, c) exchanging only one nucleotide with its complementary site CTTATG, d) exchanging two nucleotides with their complementaries CTATAG.

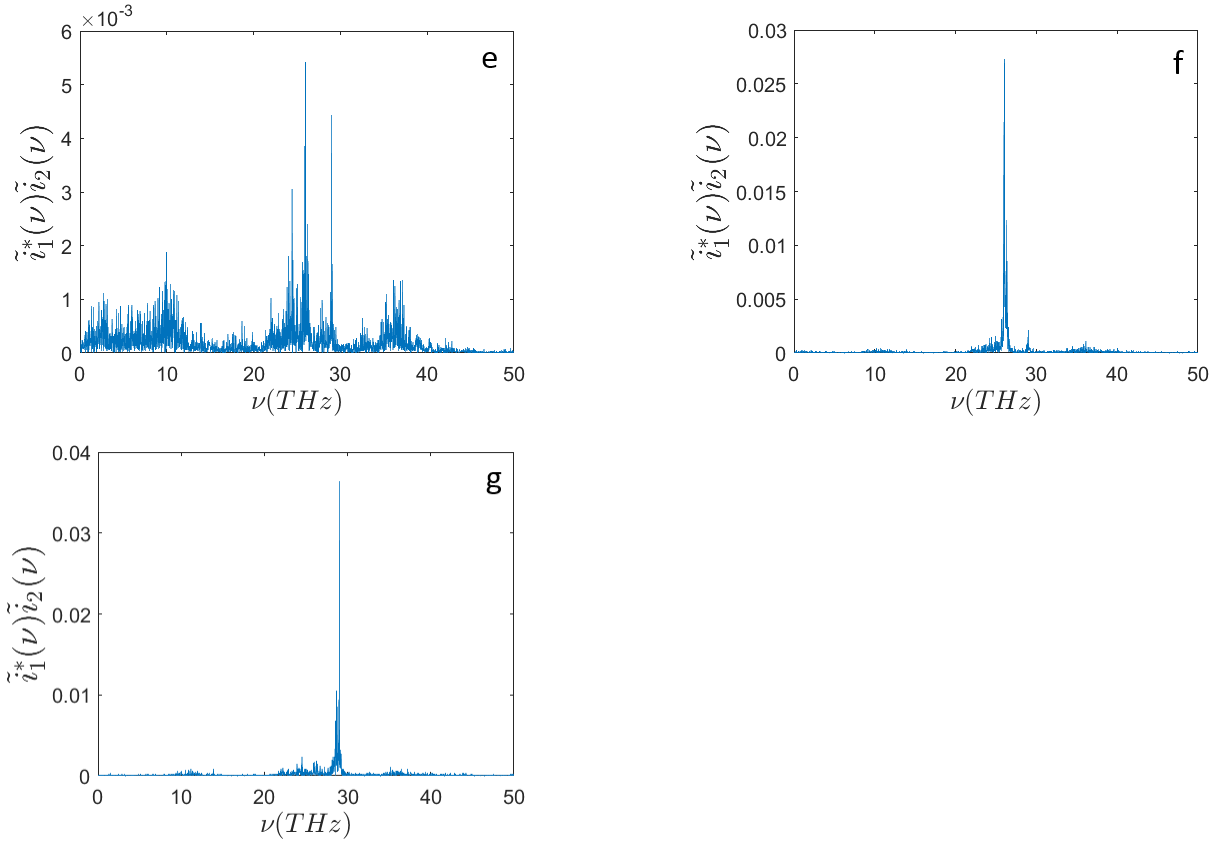

Figure 6: Same physical conditions of Figure 5. The cross frequency spectrum of the interaction between DNA and the EcoRI enzyme. e) randomized restriction sites AGATCT, f) exchanging only one nucleotide with its complementary site CATAAG, g) exchanging two nucleotides with their complementaries GT-TATG. The frequency ν is measured in $10^{13}\mathrm{s}^{-1}$.

VI. POSSIBLE MECHANISMS ACTIVATING LONG RANGE DNA-ENZYME INTERACTION

In principle, the results reported in the preceding section can be at the origin of a selective electrodynamic interaction between DNA and enzyme. In order to assess the actual relevance in biological contexts of the co-resonance of electron currents, a quantitative estimate of the strength of the implied interaction requires to work out a similar approach to the one reported in [12] from the analytical viewpoint, and to get experimental information about the intensity of the currents and the possible mechanisms of their activation in a biological environment. These points will be tackled in future investigations, in what follows we qualitatively sketch possible scenarios to activate electrodynamic DNA-enzyme interaction.

First, given two electron currents $j^{(1)}(\mathbf{x},t)$ and $j^{(2)}(\mathbf{x},t)$, representing those of DNA and

EcoRI, respectively

$$\vec{j}^{(1,2)}(\mathbf{x},t) = \frac{e\hbar}{2m_e i}\left(\psi^\star\vec{\nabla}\psi - \psi\vec{\nabla}\psi^\star\right)$$

according to the D'Alembert equations (in Gaussian units and Lorenz gauge)

$$\Box^2\vec{A}^{(1)}(\mathbf{x},t) = (4\pi/c)\vec{j}^{(1)}(\mathbf{x},t)$$

and

$$\Box^2\vec{A}^{(2)}(\mathbf{x},t) = (4\pi/c)\vec{j}^{(2)}(\mathbf{x},t)$$

the mutual interaction is described by the coupling terms

$$\vec{j}^{(2)}(\mathbf{x},t)\cdot\vec{A}^{(1)}(\mathbf{x},t) \qquad \text{and} \qquad \vec{j}^{(1)}(\mathbf{x},t)\cdot\vec{A}^{(2)}(\mathbf{x},t)\ .$$

Since the D'Alembert equation is linear, the vector potential inherits the spectral properties of the current that generates it. As a consequence, the co-resonance between the two currents $j^{(1)}(\mathbf{x},t)$ and $j^{(2)}(\mathbf{x},t)$ entails the largest values of the time averages of the interaction energies.

Second, intriguing connections exist between the models presented above, which describe electronic motions along a given DNA sequence and a given protein sequence, and the coordinated electronic fluctuations that arise from van der Waals many-body dispersion forces [18, 42–44] in a variety of molecular contexts. Specifically, productive insights have emerged from attempts to unify atomistic, continuum, and mean-field treatments in the quantum electronic behaviors of DNA and proteins in water [18, 44–47]. Even in the presence of thermally turbulent aqueous environments, it has been shown that these collective electronic dispersion correlations can persist at several nanometers from the protein-water interface, and these correlations are energetically relevant for protein folding processes at the microsecond scale [46], and likely for even longer times *in vivo*.

Kurian and coworkers [18, 42] have additionally shown that such collective electronic (Drude quantum harmonic oscillator) modes are suitably fine-tuned for the synchronized catalysis of two phosphodiester bonds ($\sim$ 0.46 eV), and that the palindromic mirror symmetry of the double-stranded DNA target sequence recognized by the enzyme (see Figure 7) allows for conservation of parity in the symmetric, site-specific cleavage of both DNA strands. By considering the radiative field $\mathbf{E}$ created by the collective electronic fluctuation modes in the DNA target sequence, a nonvanishing polarization density emerges spontaneously in the orientational correlations of the water dipole network through the interaction Hamiltonian $H = -\mathbf{d}_e\cdot\mathbf{E}$, where $\mathbf{d}_e$ is the permanent electric dipole moment for a single water molecule.

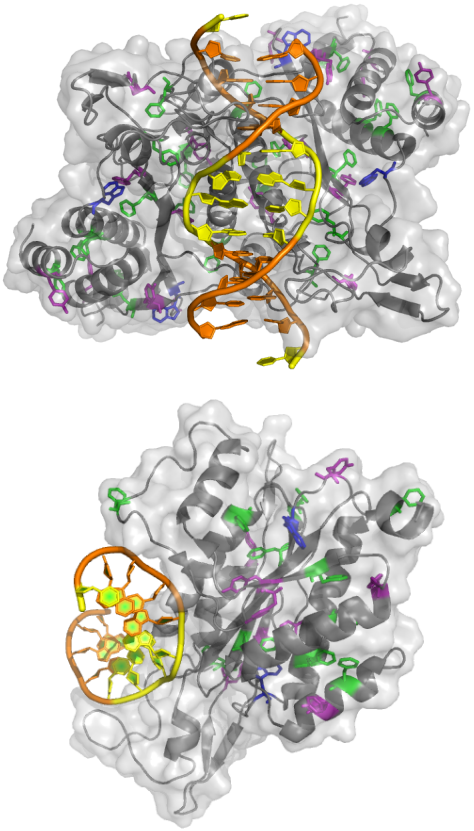

Figure 7: Aromatic network in *Eco*RI-DNA complex. Tryptophan (blue), tyrosine (purple), and phenylalanine (green) form correlated electronic dispersion networks in *Eco*RI, shown here in the top panel bound to its double-stranded DNA substrate, with adenine-thymine (yellow) and cytosine-guanine (orange) base pairs highlighted. Other amino acids (gray) are displayed in the context of their secondary structures within the enzyme, and in the bottom panel only one of the two *Eco*RI dimers is shown for clarity, to showcase the $\pi - \pi$ stacking of the DNA bases. Image of *Eco*RI (PDB ID: 1CKQ) at 1.85 Å resolution created with PyMOL and adapted from [18].

Following standard treatments in quantum optics [48], this interaction between the DNA radiative field and the surrounding (quasi-continuous) water dipole field can be written in the form of a Jaynes-Cummings-like Hamiltonian that scales with the number of water molecules N as

$$H_{\text{int}} = \hbar\sqrt{N}\gamma(a^{\dagger}S^{-} + aS^{+}), \tag{30}$$

where γ is the coupling constant proportional to the matrix element of the molecular dipole moment and inversely proportional to the volume square root, $a^{\dagger}$ and a are the creation and annihilation operators, respectively, for the DNA radiative electric field $\mathbf{E}$, and S^{+} and S^{-} are the

raising and lowering operators, respectively, for the collective water dipole state. The quasi-continuum water dipole "field" thus takes the place of the N two-level systems described in the Tavis-Cummings model [49].

It should be noted that the coupling $\sqrt{N}\gamma$ in Equation (30) between the DNA radiative field and the collective water orientational state levels [18] scales with the square root of the water density ρ, which varies with temperature and pressure. However, if we consider that the number of water molecules in a (cubic) domain encompassed by infrared wavelengths $\gtrsim 1\ \mu$m exceeds 10 billion, such sufficiently large N for the collective state can provide a protective gap against thermalization ($k_B T \approx 0.02$ eV at physiological temperatures) for the long-range correlations we consider. Furthermore, the spontaneous breakdown of phase symmetry generates a field polarization (in the so-called "limit cycle" regime) that preserves gauge invariance by dynamical coherence between the matter quasi-continuum field (DNA, water, enzyme) and the phase-locked electromagnetic field (radiative field from DNA, water, enzyme).

As a toy model, we use Faraday's law of induction for the DNA double helix, considered here as a long solenoid with radius R, n turns per unit length, and current along the backbone varying as $I = I_0 e^{-\alpha t}$, where α is in general complex. For distances from the longitudinal axis $r > R$ outside the helix-solenoid, we can estimate the induced electric field $\mathbf{E}(r,t)$ tangent to a circular path surrounding the cylindrically symmetric system:

$$|\mathbf{E}(r,t)| = \frac{\Omega}{2}\frac{|e^{-\alpha t}|}{r}, \tag{31}$$

where $\Omega = |\alpha|\mu n I_0 R^2$ and μ is the magnetic permeability in water. From Equation (31) we can thus derive the creation and annihilation operators $a^\dagger, a$ for the radiative field in the interaction Hamiltonian of Equation (30).

The resulting interaction energies range between $\sim 0.1 - 1$ eV, populating bands in the infrared spectrum between $0 < \nu < 1000$ cm^{-1}, which overlaps with the energy scale of the collective electronic fluctuation modes in the DNA target sequence and in the enzyme when taken separately, but remains distinct from the more energetic intramolecular vibrations and purely electronic transitions of individual water molecules. These collective electronic fluctuation modes in the $0.1 - 1$ eV range do not couple to the rotational quantum transitions of individual water dipoles (meV scale), but rather to the emergent polarization modes present in the collective dipole network. The spectroscopic peaks for liquid water also lie completely within this range.

Chiral sum frequency generation spectroscopy experiments [50] have demonstrated the exis-

tence of a chiral water superstructure surrounding DNA under ambient conditions, thereby confirming that the chiral structure of DNA can be imprinted electrodynamically on the surrounding solvent. These experiments have also shown that some sequence-specific fine structure persists in this chiral spine of hydration, providing a mediating context for DNA target sequence recognition by the enzyme.

VII. CONCLUDING REMARKS

The aim of the present paper is twofold. First, we put forward a novel physical interpretation for the Resonant Recognition Model (RRM) of biomolecular interactions, emerging from a widely used electron-phonon Hamiltonian applied to alternating currents along the backbone of specific DNA target sequences. Second, the work here reported contributes to the still wide open discussion of long-distance electrodynamic intermolecular interactions, which have recently been demonstrated [16, 19].

Regarding the first aim, the RRM has produced phenomenologically interesting outcomes since its conceptualization in the early '80s. The RRM in its original formulation was applied to the pair of partners of the biochemical reaction involving a DNA fragment and a restriction enzyme, EcoRI, that binds to a specific subsequence of the DNA fragment to cleave it. The interaction energies of an electron with the sequence of nucleotides composing a specific DNA fragment on the one side, and the interaction energies of an electron with the sequence of amino acids composing the EcoRI enzyme on the other side, yield two numerical sequences. The product of their Fourier spectra, or cross-spectrum, displays a sharp peak. The peak so found qualitatively witnesses to the specific relationship between the two biomolecules, though the physics behind this co-resonance still needs to be clarified. Such a clarification is provided by the co-resonance of the time-domain Fourier spectra of the alternating electron currents moving along the DNA and enzyme, respectively. These currents are worked out through quantum dynamical models describing the electron-phonon coupling, derived from standard Davydov and Holstein-Fröhlich treatments [33–35]. The remarkable finding is the disappearance of the co-resonance peak when the six-base-pair (bp) target recognition subsequence GAATTC on the DNA is randomized in different ways.

Regarding the second aim of the paper, the prospective relevance for biology of long-range selective and attractive intermolecular interactions was discussed in the Introduction and has recently

been given experimental confirmation [16] in the presence of collective intramolecular oscillations. The question naturally arises whether the electronic degrees of freedom of electrodynamically interacting molecules can offer alternative or complementary mechanisms to activate such long-range intermolecular forces. We have presented a first step in this second direction, and the remarkable finding mentioned above motivates further investigations. In fact, at present we have considered the motion of a single electron, but we can think that under suitable excitation processes (for example, under repeated ATP hydrolysis events or near an ionic channel) definitely stronger currents can be activated, producing either direct electrodynamic current-to-current interactions, or, as intriguingly proposed in [18] and discussed in the preceding section, water-mediated electrodynamical interactions between the radiative field emerging from electronic fluctuational motions in DNA and in protein, and the water dipole (matter) field in the quasi-continuum limit. Finally, the observed sequence-dependent co-resonance phenomenology for the chosen biochemical model is suggestive of a potentially rich variety of selective electrodynamic interactions of more general kind, like, for example, of DNA molecules and transcription factors under the action of electron excitation.

Acknowledgments

E.F. warmly thanks the Fondazione Cassa di Risparmio di Firenze for having co-funded her PhD fellowship. P.K. acknowledges support from the U.S.-Italy Fulbright Commission, the National Science Foundation, and the Whole Genome Science Foundation. M.P. participated in this work within the framework of the project MOLINT which has received funding from the Excellence Initiative of Aix-Marseille University - A*Midex, a French "Investissements d'Avenir" programme. R. F. acknowledges the support received by the National Group of Mathematical Physics (GNFM-INdAM), and the support from the QuantERA ERA-NET Co-fund 731473 (Project Q-CLOCKS).

[1] M. Gori, I. Donato, E. Floriani, I. Nardecchia, and M. Pettini, *Random walk of passive tracers among randomly moving obstacles*, Theor. Biol. and Med. Modelling **13**, 13 (2016).

[2] S. F. Banani, H. O. Lee, A. A. Hyman, M. K. Rosen, *Biomolecular condensates: Organizers of cellular biochemistry*, Nat. Rev. Mol. Cell Biol.**18**, 285 (2017).

[3] J. Berry, C. P. Brangwynne, M. Haataja, *Physical principles of intracellular organization via active and passive phase transitions*, Rep. Prog. Phys. **81**, 046601 (2018).

[4] L. J. Sweetlove, A. R. Fernie, *The role of dynamic enzyme assemblies and substrate channelling in metabolic regulation*, Nat. Commun.**9**, 2136 (2018)

[5] O. I. Kulaeva, E. V. Nizovtseva, Y. S. Polikanov, S. V. Ulianov, V. M. Studitsky, *Distant activation of transcription: Mechanisms of enhancer action*, Mol. Cell. Biol. **32**, 4892 (2012).

[6] J. Wang, X. Meng, H. Chen, C. Yuan, X. Li, Y. Zhou, M. Chen, *Exploring the mechanisms of genome-wide long-range interactions: Interpreting chromosome organization*, Brief. Funct. Genomics **15**, 385 (2016).

[7] Barton, P. Atanassov, M. Sigman, *Substrate channelling as an approach to cascade reactions*, Nat. Chem. **8**, 299 (2016).

[8] H. Fröhlich, *Long Range Coherence and Energy Storage in Biological Systems*, Int. J. Quantum Chem. **2**, 641 (1968).

[9] H. Fröhlich, *The Extraordinary Dielectric Properties of Biological Materials and the Action of Enzymes*, Proc. Nat. Acad. Sci. **72**, 4211 (1975).

[10] H. Fröhlich, *Log-range Coherence in Biological Systems*, Rivista Nuovo Cimento **7**, 399 (1977).

[11] H. Fröhlich, *Evidence for Coherent Excitation in Biological Systems*, Int. J. Quantum Chem. **23**, 1590 (1983).

[12] J. Preto, M. Pettini and J. Tuszynski, *On the role of electrodynamic interactions in long-distance biomolecular recognition*, Phys. Rev E**91**, 052710 (2015).

[13] I. Nardecchia, M.Lechelon, M. Gori, I. Donato, E. Floriani, S. Jaeger, S. Mailfert, D. Marguet, P. Ferrier, and M. Pettini, *Detection of long-distance electrostatic interactions between biomolecules by means of Fluorescence Correlation Spectroscopy*, Phys. Rev. E**96**, 022403 (2017).

[14] I. Nardecchia, L. Spinelli, J. Preto, M. Gori, E. Floriani, S. Jaeger, P. Ferrier, and M. Pettini, *Experimental detection of long-distance interactions between biomolecules through their diffusion behavior:*

Numerical study, Phys. Rev. E**90**, 022703 (2014).

[15] I. Nardecchia, J. Torres, M. Lechelon, V. Giliberti, M. Ortolani, Ph. Nouvel, M. Gori, Y. Meriguet, I. Donato, J. Preto, L. Varani, J. Sturgis, and M. Pettini, *Out-of-equilibrium collective oscillation as phonon condensation in a model protein*, Phys. Rev. X**8**, 031061 (2018).

[16] M. Lechelon, Y. Meriguet, M. Gori, I. Nardecchia, E. Floriani, S. Ruffenach, D. Coquillat, F. Teppe, S. Mailfert, D. Marguet, P. Ferrier, L. Varani, J. Sturgis, J. Torres, and M. Pettini, *Experimental evidence for long-distance electrodynamic intermolecular forces*, Sci. Adv. **8**, eabl5855 (2022), https://www.science.org/doi/epdf/10.1126/sciadv.abl5855

[17] I. Cosic, *Macromolecular Bioactivity: Is It Resonant Interaction Between Macromolecules? - Theory and Applications*, IEEE Transact. on Biomed. Engineering **41**,1101 (1994).

[18] P. Kurian, A. Capolupo, T. J.A. Craddock, G. Vitiello, *Water-Mediated Correlations in DNA-Enzyme Interactions*, Physics Letters A **382**, 33 (2018).

[19] M. Buchanan, *The long reach of dipoles*, Nature Phys. **18**, 366 (2022).

[20] I. Cosic, *The Resonant Recognition Model of Macromolecular Bioactivity: Theory and Applications*, (Birkhauser Verlag, Basel 1997).

[21] I. Cosic, D. Cosic, *Macromolecular Resonances*. In: Bandyopadhyay A., Ray K. (eds) *Rhythmic Oscillations in Proteins to Human Cognition*, Studies in Rhythm Engineering **1**, 11 (Springer, Singapore, 2021).

[22] I. Cosic, K. Lazar, D. Cosic, *Prediction of Tubulin resonant frequencies using the Resonant Recognition Model (RRM)*, IEEE Trans. on NanoBioscience **12**, 491 (2015).

[23] I. Cosic, D. Cosic, K. Lazar, *Is it possible to predict electromagnetic resonances in proteins, DNA and RNA?*, Nonlinear Biomedical Physics **3**, 5 (2015).

[24] I. Cosic, D. Cosic, *The Treatment of Crigler-Najjar Syndrome by Blue Light as Explained by Resonant Recognition Model*, EPJ Nonlinear Biomed. Phys. **4**, 9 (2016).

[25] I. Cosic, D. Cosic, Influence of Tuning Element Relief Patches on Pain as Analyzed by the Resonant Recognition Model. IEEE Transactions on NanoBioscience **16**, 822 (2017).

[26] I. Cosic, D. Cosic, K. Lazar, *Environmental Light and Its Relationship with Electromagnetic Resonances of Biomolecular Interactions, as Predicted by the Resonant Recognition Model*, Int. J. of Environ. Res. and Public Health **13**, 647 (2016).

[27] V. Vojisavljevic, E. Pirogova, I. Cosic, *The Effect of Electromagnetic Radiation (550nm-850nm) on I-Lactate Dehydrogenase Kinetics*, Internat. J. Radiat. Biol. **83**, 221 (2007).

[28] B.T. Dotta, N.J. Murugan, L.M. Karbowski, F.M. Lafrenie, M.A. Persinger, *Shifting wavelength of ultraweak photon emissions from dying melanoma cells: their chemical enhancement and blocking are predicted by Cosic's theory of resonant recognition model for macromolecules*, Naturwissenschaften **101**, 87 (2014).

[29] N.J. Murugan, L.M. Karbowski, M.A. Persinger, *Cosic's Resonance Recognition Model for Protein Sequences and Photon Emission Differentiates Lethal and Non-Lethal Ebola Strains: Implications for Treatment*, Open Journal of Biophysics **5**, 35 (2014).

[30] I. Cosic, V. Paspaliaris, D. Cosic, *Explanation of Osteoblastic Differentiation of Stem Cells by Photo Biomodulation Using the Resonant Recognition Model*, Appl. Sci. **9**, 1979 (2019).

[31] S. Yomosa, *The Exciton in Protein*, Journal of the Physical Society of Japan **18**,1494 (1963).

[32] U. Kettlin, A. Koltermann, P. Schwille, and M. Eigen, *Real-time enzyme kinetics monitored by dual-color fluorescence cross-correlation spectroscopy*, Proc. Natl. Acad. Sci. USA **95**, 1416 (1998).

[33] A. Scott, *Davydov's soliton*, Physics Reports **217**, 1 - 67 (1992).

[34] H. Fröhlich, *Electrons in lattice fields*, Adv. Phys. **3**, 325 - 361 (1954).

[35] T. Holstein, *Studies of polaron motion: Part I. The molecular-crystal model* , Ann. Phys. (USA) **8**, 343 - 389 (1959).

[36] E. Faraji; R. Franzosi; S. Mancini; M. Pettini, *Energy transfer to the phonons of a macromolecule through light pumping*, Sci. Rep. **11**, 6591 (2021).

[37] I. Cosic, *Macromolecular Bioactivity: Is It Resonant Interaction Between Macromolecules? - Theory and Applications*, IEEE Transact. on Biomed. Engineering **41**,1101 (1994); I. Cosic, *The Resonant Recognition Model of Macromolecular Bioactivity: Theory and Applications*, Birkhauser Verlag, Basel, (1997).

[38] V. Veljkovic and I. Slavic, *General model of pseudopotentials*, Phys. Rev. Lett. **29**,105 - 108 (1972).

[39] M. B. Hakim, S. M. Lindsay, and J. Powell, *The speed of sound in DNA*, Biopolymers: Original Research on Biomolecules, **23**, 1185 (1984).

[40] L. Cruzeiro, J. Halding, P. L. Christiansen, O. Skovgaard, A. C. Scott, (1988). *Temperature effects on the Davydov soliton*, Phys. Rev. A, **37**, 880 (1988).

[41] A. Scott, *Davydov soliton*, Phys. Rep. **217**, 1- 67 (1992).

[42] Kurian, P.; Dunston, G.; Lindesay, J. How Quantum Entanglement in DNA Synchronizes Double-Strand Breakage by Type II Restriction Endonucleases. Journal of Theoretical Biology 2016, 391, 102?112. https://doi.org/10.1016/j.jtbi.2015.11.018.

[43] Hermann, J.; Alfé, D.; Tkatchenko, A. Nanoscale $\pi - \pi$ Stacked Molecules Are Bound by Collective Charge Fluctuations. Nature Communications 2017, 8, 14052. https://doi.org/10.1038/ncomms14052.

[44] M. Gori, P. Kurian, and A. Tkatchenko. Second quantization approach to many-body dispersion interactions. In submission with *Physical Review Letters* (2022).

[45] Kurian, P. Chirality-Energy Conversion Induced by Static Magnetic Effects on Free Electrons in Quantum Field Theory. Journal of Physics Communications 2018, 2 (11), 111002. https://doi.org/10.1088/2399-6528/aae876.

[46] Stöhr, M.; Tkatchenko, A. Quantum Mechanics of Proteins in Explicit Water: The Role of Plasmon-like Solute-Solvent Interactions. Science Advances 2019, 5 (12), eaax0024. https://doi.org/10.1126/sciadv.aax0024.

[47] Kurian, P. From Micro to Macro: A Relativistic Treatment of the Chiral Energy Shifts Caused by Static Electromagnetic Effects on Free Electrons. Entropy 2022, 24 (3), 358. https://doi.org/10.3390/e24030358

[48] C.C. Gerry and P.L. Knight, Introductory Quantum Optics, Cambridge UP (2005).

[49] Tavis, M.; Cummings, F. W. Exact Solution for an N -Molecule–Radiation-Field Hamiltonian. Phys. Rev. 1968, 170 (2), 379?384. https://doi.org/10.1103/PhysRev.170.379.

[50] McDermott, M. L.; Vanselous, H.; Corcelli, S. A.; Petersen, P. B. DNA's Chiral Spine of Hydration. ACS Central Science 2017, 3 (7), 708-714. https://doi.org/10.1021/acscentsci.7b00100.